ELSEVIER

Journal of Atmospheric and Solar-Terrestrial Physics 69 (2007) 2238–2248

Journal of ATMOSPHERIC AND SOLAR-TERRESTRIAL PHYSICS

www.elsevier.com/locate/jastp

The global distribution of gravity wave energy in the lower stratosphere derived from GPS data and gravity wave modelling: Attempt and challenges

K. Fröhlich[a,*], T. Schmidt[b], M. Ern[c], P. Preusse[c], A. de la Torre[d], J. Wickert[b], Ch. Jacobi[a]

[a]*Institut für Meteorologie, Universität Leipzig, Stephanstr. 3, D-04103 Leipzig, Germany*
[b]*Department 1: Geodesy and Remote Sensing, Geoforschungszentrum Potsdam, Germany*
[c]*Institute for Chemistry and Dynamics of the Geosphere, Forschungszentrum Jülich, Germany*
[d]*Facultad de Ciencias Exactas y Naturales, Universidad Buenos Aires, Argentina*

Received 24 January 2007; received in revised form 15 June 2007; accepted 14 July 2007
Available online 24 July 2007

Abstract

Five years of global temperatures retrieved from radio occultations measured by Champ (Challenging Minisatellite Payload) and SAC-C (Satelite de Aplicaciones Cientificas-C) are analyzed for gravity waves (GWs). In order to separate GWs from other atmospheric variations, a high-pass filter was applied on the vertical profile. Resulting temperature fluctuations correspond to vertical wavelengths between 400 m (instrumental resolution) and 10 km (limit of the high-pass filter). The temperature fluctuations can be converted into GW potential energy, but for comparison with parameterization schemes GW momentum flux is required. We therefore used representative values for the vertical and horizontal wavelength to infer GW momentum flux from the GPS measurements. The vertical wavelength value is determined by high-pass filtering, the horizontal wavelength is adopted from a latitude-dependent climatology. The obtained momentum flux distributions agree well, both in global distribution and in absolute values, with simulations using the Warner and McIntyre parameterization (WM) scheme. However, discrepancies are found in the annual cycle. Online simulations, implementing the WM scheme in the mechanistic COMMA-LIM (Cologne Model of the Middle Atmosphere—Leipzig Institute for Meteorology) general circulation model (GCM), do not converge, demonstrating that a good representation of GWs in a GCM requires both a realistic launch distribution and an adequate representation of GW breaking and momentum transfer.

Keywords: Gravity waves; Momentum flux; Parameterization scheme; GPS

1. Introduction

The physical description of gravity waves (GWs) in general circulation models (GCMs) is still based on parameterizations, since GWs are still of too small scale to be resolved on a global grid, but altogether they impose a huge amount of momentum in

*Corresponding author. Tel.: +49 341 97 32875; fax: +49 341 97 32899.
E-mail address: kfroehlich@uni-leipzig.de (K. Fröhlich).

1364-6826/$ - see front matter © 2007 Elsevier Ltd. All rights reserved.
doi:10.1016/j.jastp.2007.07.005

the mesopause region, which changes the background circulation and leads to an extremely cold summer polar mesopause (e.g. Lübken and Müllemann, 2003; Lübken et al., 2004). A large number of approaches of vertical wave propagation and wave breaking has been implemented into current middle atmosphere models. It is still difficult to describe the whole spectrum of GWs, which in frequency space varies from the Brunt–Väisälä frequency N to the Coriolis parameter f, and covers a broad band of wavelengths in both the horizontal and vertical domains.

Satellite observations are in principle well suited for a global detection of GW activity; however, due to their physically limited resolution, limb sounding satellites cannot detect waves with horizontal wavelengths $\lambda_x < 100$ km (Preusse et al., 2002, Lange and Jacobi, 2003). Further, the coarse sampling rates of most satellite measurements do not allow deducing any horizontal wavelength information. Horizontal wavelength information, however, is required to infer momentum flux. The lack of horizontal wavelength information is particularly problematic in the tropics where large-amplitude waves with long horizontal scales dominate and may mask shorter-scale waves generated by distinct sources even if these carry larger momentum.

Momentum flux, in turn, is the primary variable in GW parameterization schemes. CRISTA satellite measurements have shown (Ern et al., 2004, 2006) that at the equator GW potential energy is maximum, but momentum flux is minimum. This is due to the prevalence of low-frequency, large horizontal wavelength GWs in the tropics (Alexander et al., 2002; Ern et al., 2004; Preusse et al., 2006). The relevant quantity that is used to include the effect of GWs in the model dynamics is momentum flux and should therefore be the quantity to be compared with measurements (see also Ern et al., 2006). Recently, Ern et al. (2006) have compared absolute values of GW momentum flux deduced from the two CRISTA missions (November 1994 and August 1997) with simulations employing the Warner and Mclntyre (WM) scheme. By varying tuneable parameters they found in particular that the satellite data only could be matched for a low launch altitude of GWs in the WM scheme (<6 km). The study of Ern et al. (2006) considers longer vertical wavelengths (5–30 km) and covers 2 single weeks, only. They found that the WM scheme overestimated the summer mid- and high latitudes at the upper measurement boundary of 45 km.

In a study of global positioning system (GPS) radio occultation (RO) data presented in this paper, we focus on very short vertical wavelengths (<10 km) and consider a 5-year data set. For the shorter vertical wavelengths we expect such kinds of overestimation to occur already at lower altitudes. The GPS-RO data can therefore be used to confirm the results of Ern et al. (2006) and to test whether the summer mid-latitude difference is a typical feature or a particularity occurring only in the one week of the second CRISTA mission. The paper is organized as follows: Section 2 introduces the data and the analysis technique; Section 3 compares measurements with offline simulations using ECMWF data and the WM scheme; Section 4 uses the tuned WM scheme for an online simulation in a GCM, demonstrating that a good representation of GWs not only is required at source levels of GW activity in a GCM but also needs an adequate representation of GW breaking and momentum transfer. Section 5 summarizes the results and concludes the paper.

2. Using GPS data to estimate GW momentum fluxes

GPS-RO data obtained with the low-earth-orbit satellites CHAMP (Challenging Minisatellite Payload) and SAC-C (Satelite de Aplicaciones Cientificas-C) during the last 5 years were used to derive temperature profiles and subsequently temperature disturbances. For this purpose, the profiles were binned into $10^\circ \times 10^\circ$ wide grid boxes. The average monthly number of profiles in each grid box is about 6–10, leading to an approximate total number of 30–50 profiles per grid box in the 5-year average. The data set was checked out if the vertical profiles fulfilled the condition of a positive vertical gradient of potential temperature $\partial\theta/\partial z > 0$ in the lower stratosphere, which was the case for about 99% of all profiles. The mean specific potential energy (per unit mass)

$$E_{\mathrm{P}} = g^2 \hat{T}^2/(2N^2T^2) \tag{1}$$

as a measure of the total energy related with GW activity (GWA) depends on the vertical wavelength λ_z and involves an integral over a vertical column equal to one wavelength:

$$E_{\mathrm{P}\lambda_z} = \lambda_z^{-1} \int_0^{\lambda_z} E_{\mathrm{P}}\, \mathrm{d}z. \tag{2}$$

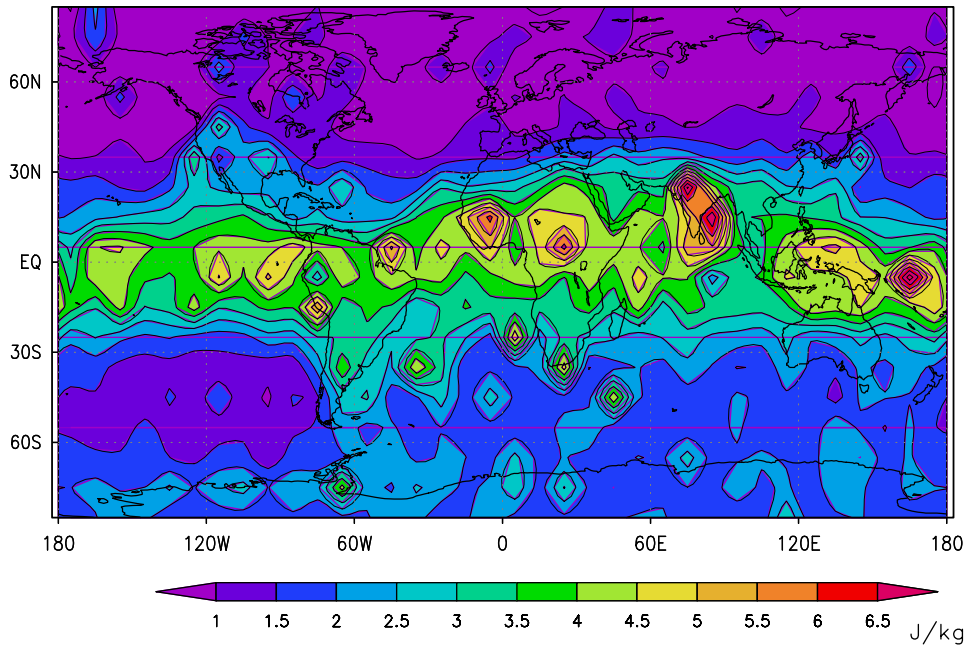

Fig. 1. July 2001–2005 average of the mean global potential energy distribution for vertical wavelengths between 4 and 10 km integrated over a layer between 19 and 29 km.

Here, g represents the acceleration due to gravity, T is the background temperature, $\hat{T}$ is the temperature amplitude of the gravity wave, and N is Brunt–Väisälä frequency. In order to avoid an influence of the GWs on N itself the Brunt–Väisälä frequency N was obtained from the filtered background temperature.

An algorithm described in de la Torre et al. (2006) was applied in order to filter the data for different vertical wavelengths with an upper cut-off at 10 km. Only data above the tropopause were used. The layers of integration in the lower stratosphere vary between 10 and 30 km in order to obtain a detailed view there. Now 5 years of monthly mean GWA are available. It is important to note that the activity seen by the satellites does not cover the whole spectrum of GWs. Due to the sampling rate and viewing angles especially at low latitudes only relatively slowly upward-propagating waves and waves with large horizontal wavelengths dominate (Alexander et al., 2002; Lange and Jacobi, 2003). In addition, in particular Kelvin waves are likely to be included in the signal since the data were not filtered by their zonal wave numbers. In order to present a multi-year average of GWA and to perform calculations on the global data, the existing data gaps were closed by taking an average of the surrounding occupied values.

Fig. 1 shows the 2001–2005 mean July mean E_p integrated between 19 and 29 km, in units of J/kg. The most prominent feature is the strong GWA around the tropics and subtropics. Three distinct spots appear over Africa, India and the South-Eastern Pacific. Furthermore, at middle and high latitudes GWA is higher in the winter (southern) hemisphere than in the summer hemisphere. This feature was expected (e.g. McLandress et al., 2000; Preusse et al., 2004; Ratnam et al., 2004); however, the extreme low values in the summer hemisphere raise the question from where the momentum fluxes and subsequent accelerations on the mean flow in the summer mesosphere originate. Is this due to the limited part of the GWs, which can be seen in the stratosphere, or does slant wave propagation play a role?

If we would like to compare the values with model data, knowledge of momentum fluxes is required. Following Ern et al. (2004), under mid-frequency approximation of the considered GWs, the potential energy can be related to the horizontal momentum flux F_h via the ratio of the horizontal and vertical wave numbers k and m:

$$F_{\mathrm{h}} = \frac{1}{2}\rho\frac{k}{m}\left(\frac{g}{N}\right)^2\left(\frac{\hat{T}}{T}\right)^2 = \rho\frac{k}{m}E_{\mathrm{P}}, \tag{3}$$

where ρ is atmospheric density (note the unit changed now to Pa). The global maps of E_P contain GWA in a 10 km interval at wavelengths between 4 and 10 km; therefore the vertical wavelength $\lambda_z = 5$ km should be well represented. However, the horizontal wavelength necessary to calculate F_h needs some consideration. Using results of Preusse et al. (2006) and in consideration of the need for a representative and not an upper limit horizontal wavelength, we set the ratio of intrinsic frequency to the Coriolis parameter $\hat{\omega}/f = 3$. Using the mid-frequency approximation for the intrinsic frequency $\hat{\omega}$ we obtain $k = 3fm/N$ as a measure for the horizontal wave number; thus

$$\frac{k}{m} = 3\frac{f}{N}, \tag{4}$$

which may be used in Eq. (3). However, for small latitudes (i.e. close to the equator) k approaches zero and the horizontal wavelength becomes infinite. This is unphysical. CRISTA observations in the tropics indicate a typical horizontal wavelength of ~1500 km for a vertical wavelength of <10 km (Preusse et al., 2006) and we use this value for all latitudes where Eq. (4) would result in larger horizontal wavelengths. The typical horizontal wavelength is therefore deduced from the observations at all latitudes and is described by Eq. (4) in the extra-tropics and by the constant value of 1500 km in the tropics. Making these rough estimates provides a means to derive the momentum flux of GWs from the satellite data. A first check as to whether the obtained values represent real conditions was made by comparing the August mean momentum flux (not shown here) with CRISTA values (Ern et al., 2004). An overall agreement was found. However, due to different years and time-averaging scales these pictures could not be identical. In addition, the visibility interval for vertical wavelengths is shifted towards longer wavelengths in the CRISTA data.

In order to investigate the behavior of momentum flux during the year, in Fig. 2 momentum flux values obtained from GPS-RO for different seasons are shown. They show the expected maxima and minima and some interesting additional features. For instance, the spot over India during boreal summer (panel c) remains and there is also a spot of GWA at the Antarctic Peninsula at this time. The strongest activity is found for January in the winter hemisphere, while the month of July exhibits much lower values around the South Pole. In the southern hemisphere large activity can be found during October. Again, summer hemispheric values of gravity wave momentum fluxes are extremely low.

The spotty structure in all maps was found to appear quite regularly during the 5 years and its reliability is also supported by the quality check of the original data. However, one has to note that the grid boxes are non-overlapping. Overlapping grid boxes smooth the maps, but we expected to gain a better identification of geographic contributions, avoiding contamination from adjacent cells. The size of the grid boxes is a compromise between resolving localized forcing regions and providing a climatological mean. High intermittency of GW variances is reported from other instruments, for instance from CRISTA (Preusse et al., 1999, 2003). Adjacent profiles (miss distance of a few hundred km) measured during a single day can differ in GW variance by more than an order of magnitude. This leads to single grid boxes with enhanced values in the maps, as shown in Figs. 1 and 2.

3. Offline calculations with the Warner–Mcintyre scheme

The next step was to investigate whether a GW drag scheme is able to reproduce the properties presented in Section 2. For this purpose the WM scheme was used. This scheme uses a simple spectral approach for GWs under mid-frequency approximation and describes their upward propagation and breaking by considering the behavior of the saturated and unsaturated parts of the vertical wave number spectrum (Warner and McIntyre, 2001). In order to simulate a satellite view on the GWs a visibility filter was applied. This means that only vertical wavelengths smaller 10 km were used, while the horizontal wavelength was allowed to vary within 150 km and 40000 km $\times \cos\varphi$ according to the satellite λ_x-range the data contain. Additionally, the GW spectrum was initialized with optimum launching parameters as, for instance, a saturated vertical wave number $m^* = 1/3$ cycles/km, a slope of the unsaturated vertical wave number spectrum $s = 2$ and a launching height at about 5 km. These values are taken from Ern et al. (2006), who applied the WM scheme to compare absolute values of GW momentum flux deduced from the two CRISTA missions. The launch height in the troposphere provides a longitudinal filtering particularly due to the subtropical jets. This cannot be achieved if the

GWs are launched in the lower stratosphere. In the WM scheme the total gravity wave energy (potential plus kinetic energy) at the launch level is assumed to have a constant value E_0 independent of its location (Fritts and VanZandt, 1993; Warner and McIntyre, 1996). Since the frequency spectrum of the total wave energy $B(\hat{\omega}) = B_0 * \widehat{\omega}^{-p}$ is normalized to unity and the GW momentum flux launch spectrum has a $\hat{\omega}^{1-p}$ dependency, this assumption leads to a latitudinal (symmetrical) dependence of the GW momentum flux at the launch level roughly of the form $\hat{\omega}_{\min}^{2/3}$. This minimum intrinsic frequency is

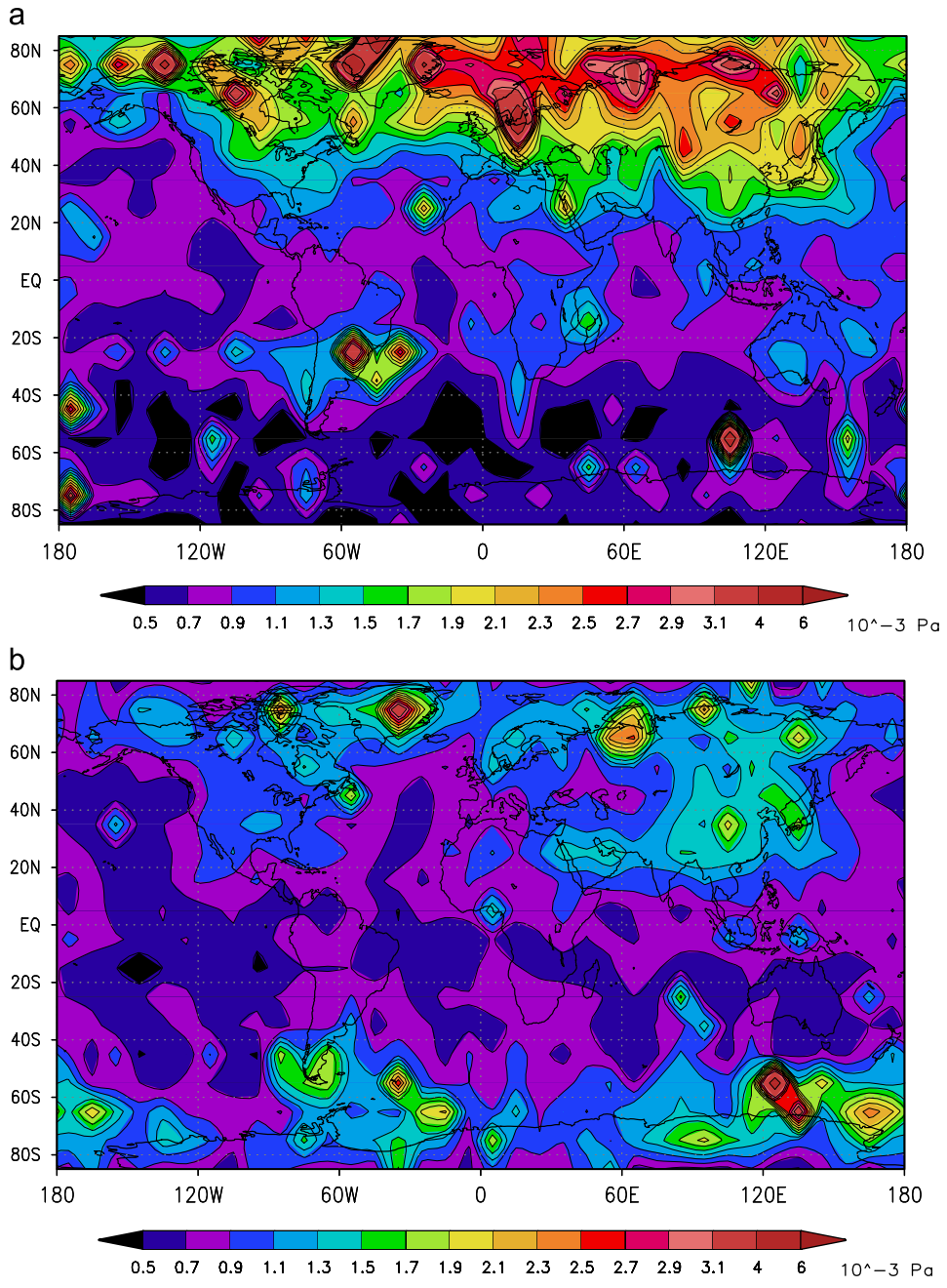

Fig. 2. Seasonal behavior of momentum flux derived from GPS potential energy for the same range of vertical wavelength and height interval as given in Fig. 1. Figures show a 5-year mean between 2002 and 2006 for January (a), and between 2001 and 2005 for April (b), July (c) and October (d).

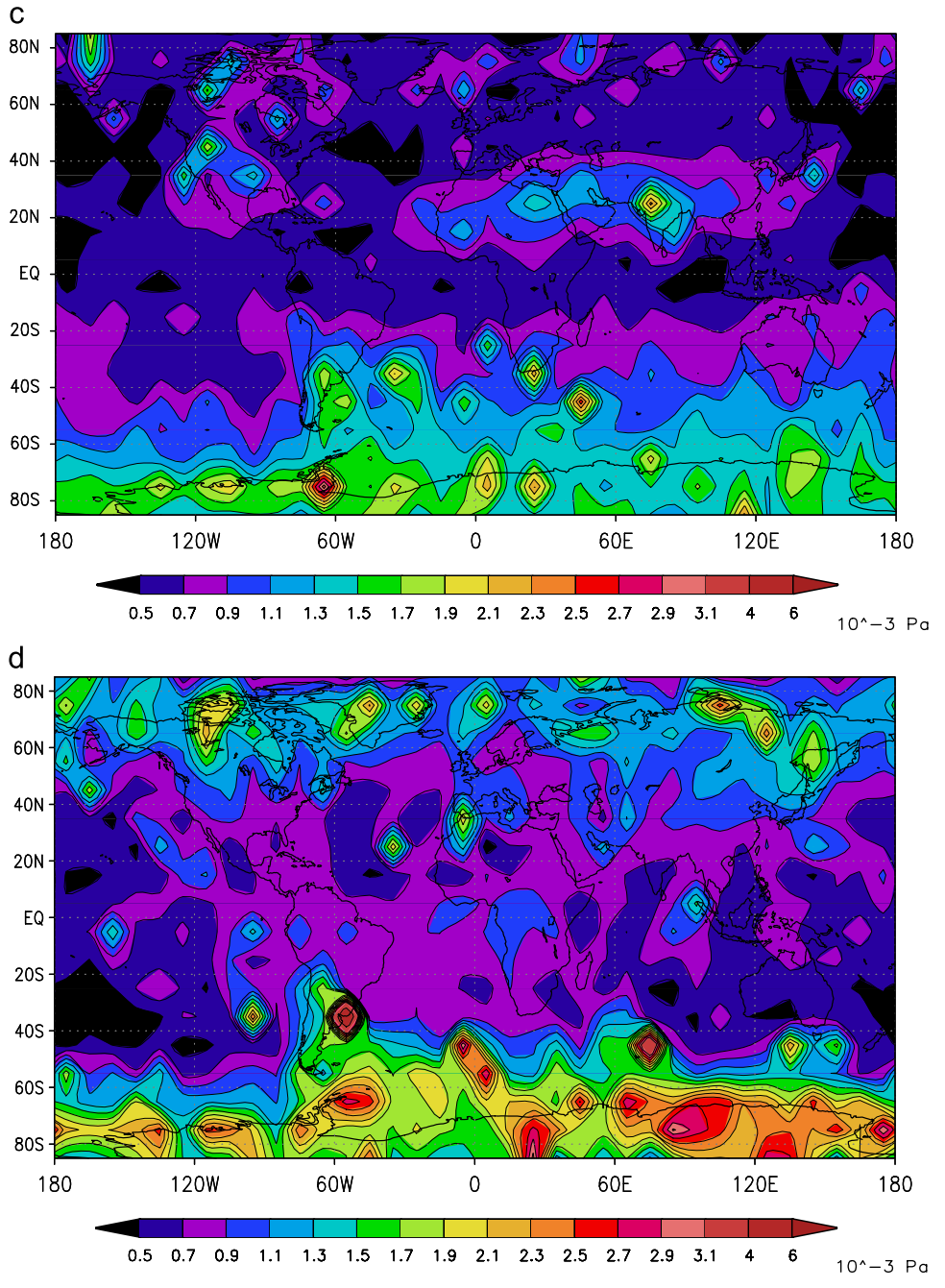

Fig. 2. (*Continued*)

given either by the Coriolis frequency or by a 'characteristic equatorial minimum frequency' (Warner and McIntyre, 1996). The longitudinal dependence is neglected.

Background conditions were provided by daily ECMWF data (12:00) within the time range from 1.1.2002 to 31.1.2006 and interpolated to the given GPS measurement times and locations. The upper boundary of the WM scheme was set to 50 km.

Fig. 3 shows the simulated seasonal GWA behavior integrated for the same height interval as applied to the GPS-RO data. The similarities are quite striking; in January (Fig. 3a) the northern hemisphere shows good agreement of structures

with enhanced values over the continents extending to polar latitudes; in the southern subtropics the three spots over South America, South Africa and Australia can be identified in both maps. In July (Fig. 3c) the monsoon pattern over India and Africa is recognized as well as the intensification of GWA in the Antarctic region. However, for solstice conditions the WM scheme shows stronger activity in the summer hemisphere than the satellite data. This feature confirms results of the study with

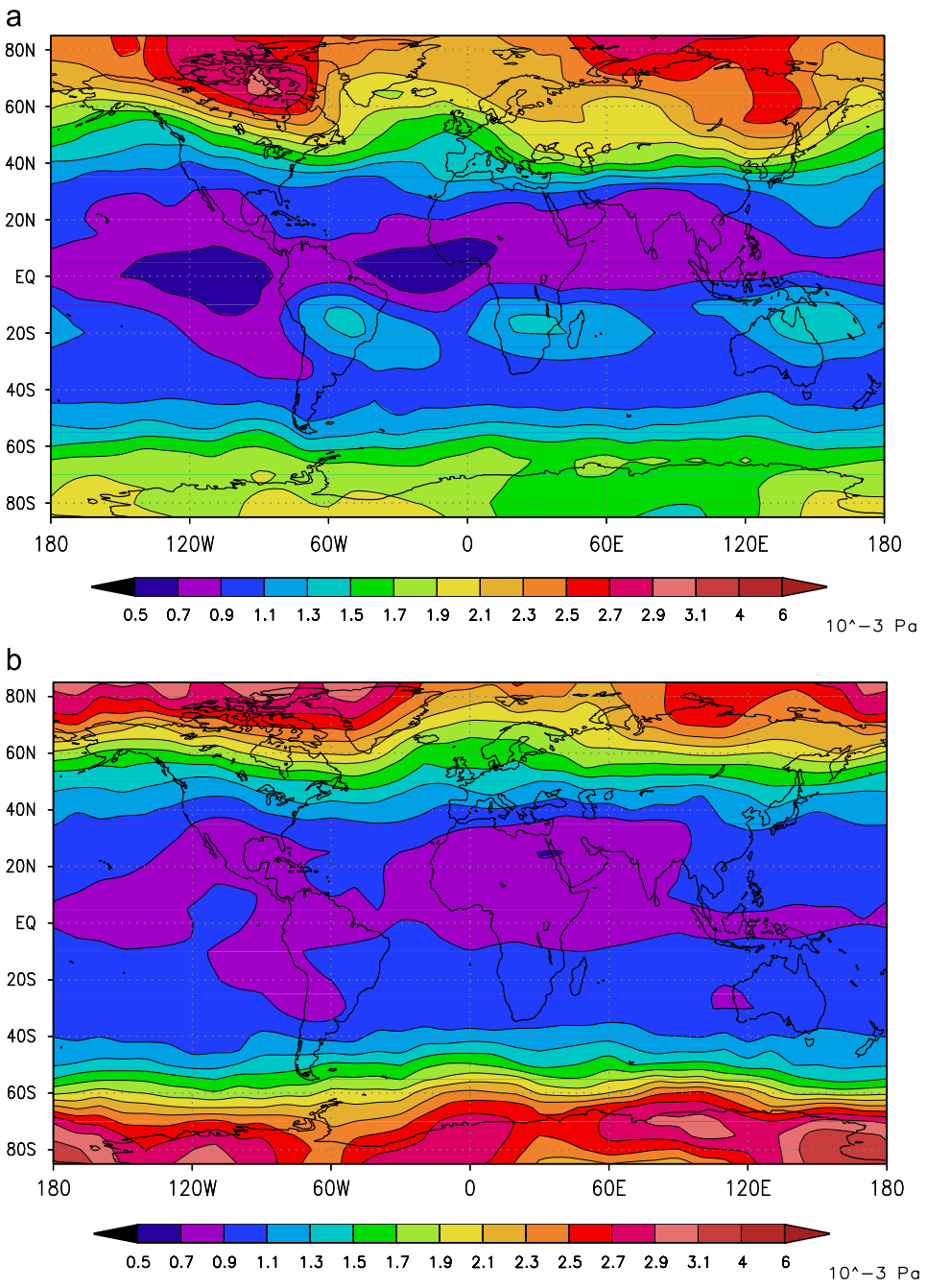

Fig. 3. Seasonal behavior of momentum flux as calculated with the visibility filtered WM scheme for the same range of vertical wavelength and height as in Fig. 2. Again, (a) January, (b) April, (c) July, and (d) October.

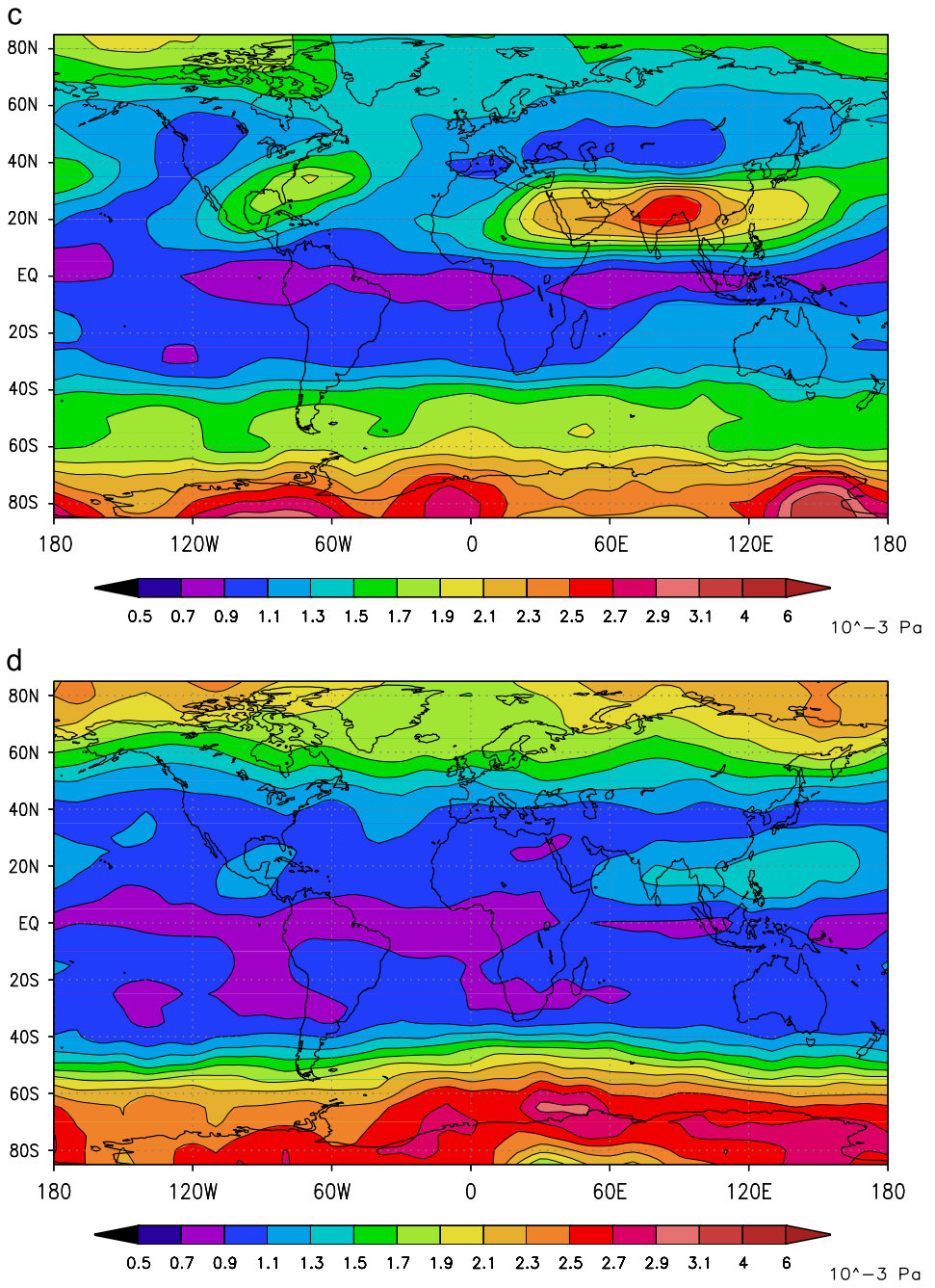

Fig. 3. (*Continued*)

CRISTA data by Ern et al. (2006), where they found an overestimation of GWA calculated by the WM scheme at summer mid- and high latitudes.

The accordance in both data sets might indicate that wind filtering plays an important role in that part of the GW spectrum since the background conditions fairly coincide.

During equinoxes the GWA in both data sets dominates at high latitudes. Both satellite and WM scheme results show that in April (Fig. 3b) the activity at northern and southern high latitudes is symmetric in structure and amplitudes while for October (Fig. 3d) the southern hemisphere activity dominates. The comparison indicates a good agree-

ment between the two data sets for the month of October (Fig. 3d) while for April the WM scheme delivers too high fluxes in comparison with the GPS-RO data. However, taking into account that the GPS momentum fluxes are derived with fairly rough information this result is quite encouraging. The question arises, since the information of a part of the GW spectrum can be modelled, whether and how this information can be used also in general circulation models.

4. Online calculations with COMMA-LIM

In order to connect the results obtained in the lower atmosphere with processes in the mesosphere–lower thermosphere region, a numerical model for the middle atmosphere is needed. COMMA-LIM (Cologne Model of the Middle Atmosphere—Leipzig Institute for Meteorology) is a simple 3D GCM. It extends up to 150 km geometrical height. The equations are solved on a spherical grid with a horizontal resolution of $5^\circ \times 5.6^\circ$ (latitude/longitude). The model describes the relevant middle atmosphere processes such as heating and cooling by the important gases—which excite the tides self-consistently, the diffusive and molecular conduction processes as well as ion drag and Lorentz deflection in ionospheric heights. Planetary waves can be forced near the tropopause by corresponding heating disturbances. At the lower boundary, geopotential and temperature fields obtained from 11-year averaged Met Office data provide a zonal mean as well as stationary planetary waves with zonal wave number 1 and 2.

The standard GW parameterization scheme is an updated Lindzen (1981) type scheme taking into account multiple breaking levels and wave propagation between layers, where the wave is saturated, as well as heating/cooling effects due to GW dissipation. The waves are forced isotropically in 8 directions starting with 6 different phase speeds $c = 5$–30 m/s, while the horizontal wavelength is fixed to 300 km. The initial vertical velocity is weighted by frequency and phase speed following Gavrilov and Fukao (1999) in order to provide a realistic spectrum at the launch height of ~10 km. In addition, a latitudinal and seasonal weighted term with higher GW activity in the winter hemisphere is applied. Vertical velocity and vertical wave number are calculated using the WKB approximation on the vertical structure equation for GWs. Wave breaking occurs in the scheme when isentropes first become vertical, thus implying a loss of static stability and the onset of turbulence and mixing. This process is expressed in terms of acceleration, heating and dissipation rates due to GWs. More details about this GW scheme in COMMA-LIM can be found in Jacobi et al. (2006).

This GW parameterization scheme is able to produce such strong accelerations that the background wind reverses. However, the calculated summer polar mesopause temperature does not reach values below 160 K where the temperature can be below 130 K (Lübken and Müllemann, 2003). This missing feature was one reason to search for other GW schemes. Tuning factors in the scheme have been switched off in order to stay in the physically reasonable range. If the physical parameterization is not able to remove the heat from the summer pole then this indicates that the scheme does not resolve all important processes.

Beside this missing feature one of the ongoing interests in model developing was the implementation of a spectral-approach GW model because it is assumed to give a better opportunity of comparing the calculated momentum fluxes to observations.

Therefore, the WM scheme was implemented into COMMA-LIM and online simulations were carried out. Several parameters were changed in order to study the effect on the model and to obtain the best result. For instance, the vertical wavelength of m^* was varied from 2 to 4 km, the slope of the unsaturated vertical wave number spectrum s was tested for $s = 1$, 1.5 and 2, and the launch height was varied from 7 to 18 km, with respect to the vertical gridpoints of COMMA-LIM. Unfortunately, it turned out that the WM scheme fails for all cases to impose the acceleration on the mesopause region that is necessary to maintain the observed circulation (not shown here).

In general, it seems that the process of GW breaking in the WM scheme starts too early and smears the momentum deposition throughout the mesosphere so that the amount of acceleration in the mesopause region is too weak. McLandress and Scinocca (2005) reported about similar problems while comparing several GW schemes. They also found that the deposition height of the WM scheme is too low to produce a reasonable response in a GCM; therefore they inserted a parameter, which increased the height of momentum deposition. However, sensitivity studies on COMMA-LIM dealing with several tuneable parameters were not successful. It has to be investigated whether there

still is a way to use the WM scheme in COMMA-LIM.

Therefore, the idea of using observational data for inclusion in and comparison with model data is problematic not only due to observational limitations but also due to modeling challenges. Online simulations using the WM scheme show that it is not sufficient alone to include measured information like better GW source conditions in the simulations. Another modelling challenge is to provide adequate GW schemes that are able to characterize the propagation and breaking processes for the whole middle atmosphere effectively and as accurately as possible.

5. Conclusions

Based on a 5-year climatology of gravity wave activity of GPS-RO measurements in the lower stratosphere, an estimation of the momentum flux was made in order to be able to compare the results to model outputs. Using offline calculations in the lower atmosphere, the WM scheme worked well in reproducing relevant patterns of GWA in the lower stratosphere during the year as has already been shown in Ern et al. (2006). Even if only a part of the whole GW spectrum can be observed it might be a first step of using observational GW data in models. However, it is questionable as to whether if the WM scheme can be used within a GCM to track the GW information upwards while describing breaking processes in the upper middle atmosphere since it fails for the standard spectrum to do so. Therefore, input from two sides is further required; on the one hand high-resolution satellite data of GWA to resolve wave properties and on the other hand spectral models that are able to simulate successfully acceleration and heating rates needed for the special behavior of the mesopause region.

Acknowledgment

This work was supported by Deutsche Forschungsgemeinschaft under grants JA836/21-1, WI2634/2-1/503976 and ER 474/1-1 within SPP1176 "CAWSES".

References

Alexander, M.J., Tsuda, T., Vincent, R.A., 2002. Latitudinal variations observed in gravity waves with short vertical wavelengths. Journal of Atmospheric Sciences 59, 1394–1404.

De la Torre, A., Schmidt, T., Wickert, J., 2006. A global analysis of wave potential energy in the lower stratosphere derived from 5 years of GPS Radio occultation data with CHAMP. Geophysical Research Letters 33, L24809.

Ern, M., Preusse, P., Alexander, M.J., Warner, C.D., 2004. Absolute values of gravity wave momentum flux derived from satellite data. Journal of Geophysical Research 109, D20103.

Ern, M., Preusse, P., Warner, C.D., 2006. Some experimental constraints for spectral parameters used in the Warner and McIntyre gravity wave parameterization scheme. Atmospheric Chemistry and Physics 6, 4361–4381.

Fritts, D.C., VanZandt, T.E., 1993. Spectral estimates of gravity wave energy and momentum fluxes. Part I: energy dissipation, acceleration and constraints. Journal of Atmospheric Sciences 50, 3685–3694.

Gavrilov, N.M., Fukao, S., 1999. A comparison of seasonal variations of gravity wave intensity observed with the middle and upper atmosphere radar with a theoretical model. Journal of Atmospheric Sciences 56, 3485–3494.

Jacobi, Ch., Fröhlich, K., Pogoreltsev, A.I., 2006. Quasi-two-day wave modulation of gravity wave flux and consequences for the planetary wave propagation in a simple circulation model. Journal of Atmospheric and Solar-Terrestrial Physics 68, 283–292.

Lange, M., Jacobi, C.h., 2003. Analysis of gravity waves from radio occultation measurements. In: Reigber, C.h., Lühr, H., Schwintzer, P. (Eds.), First CHAMP Mission Results for Gravity, Magnetic and Atmospheric Studies. Springer, Berlin, pp. 479–484.

Lindzen, R.S., 1981. Turbulence and stress owing to gravity wave and tidal breakdown. Journal of Geophysical Research 86, 9707–9714.

Lübken, F.-J., Müllemann, A., 2003. First in situ temperature measurements in the summer mesosphere at very high latitudes (78°N). Journal of Geophysical Research 108, 8448.

Lübken, F.-J., Müllemann, A., Jarvis, M., 2004. Temperatures and horizontal winds in the Antarctic summer mesosphere. J. Geophys. Res., 109, doi:10.1029/2004JD005133.

McLandress, C., Alexander, M.J., Wu, D.L., 2000. Microwave Limb Sounder observations of gravity waves in the stratosphere: a climatology and interpretation. Journal of Geophysical Research 105 (D9), 11947–11967.

McLandress, C., Scinocca, J.F., 2005. The GCM response to current parameterizations of nonorographic gravity wave drag. Journal of Atmospheric Sciences 62, 2394–2412.

Preusse, P., Schaeler, B., Bacmeister, J., Offermann, D., 1999. Evidence for gravity waves in CRISTA temperatures. Advances in Space Research 24, 1601–1604.

Preusse, P., Dörnbrack, A., Eckermann, S.D., Riese, M., Schaeler, B., Bacmeister, J.T., Broutman, D., Grossmann, K.U., 2002. Space based measurements of stratospheric mountain waves by CRISTA, 1. Sensitivity, analysis method and a case study. Journal of Geophysical Research 107, 8178.

Preusse, P., Eckermann, S.D., Ern, M., Schmidlin, F.J., Alexander, M.J., Offermann, D., 2003. Infrared limb sounding measurements of middle atmosphere gravity waves by CRISTA. SPIE Proceedings 4882, 134–148.

Preusse, P., Ern, M., Grossmann, K.U., Mergenthaler, J.L., 2004. Seasonal variations of gravity wave variance inferred from CLAES. In: Schäfer, K.P., Comeron, A., Carleer, M.R., Picard, R.H. (Eds.), Remote Sensing of Clouds and the Atmosphere VIII. Proceedings of SPIE 5235, 288–297.

Preusse, P., Ern, M., Eckermann, S.D., Warner, C.D., Picard, R.H., Knieling, P., Krebsbach, M., Russell, J.M., Mlynczak, M.G., Mertens, C.J., Riese, M., 2006. Tropopause to mesopause gravity waves in August: measurement and modelling. Journal of Atmospheric and Solar-Terrestrial Physics 68, 1730–1751.

Ratnam, M.V., Tetzlaff, G., Jacobi, Ch., 2004. Global and seasonal variations of stratospheric gravity wave activity deduced from the CHAllenging Minisatellite Payload (CHAMP)-GPS Satellite. Journal of Atmospheric Sciences 61, 1610–1620.

Warner, D.C., McIntyre, M.E., 1996. On the propagation and dissipation of gravity wave spectra through a realistic middle atmosphere. Journal of Atmospheric Sciences 53 (14), 3213–3235.

Warner, D.C., McIntyre, M.E., 2001. An ultrasimple spectral parameterization for nonorographic gravity waves. Journal of Atmospheric Sciences 58 (14), 1837–1857.